A MODEL FOR PROGNOSIS OF MANUFACTURING OF A CMOS CROSS-COUPLED VOLTAGE CONTROLLED OSCILLATOR

E.L. Pankratov

[1] Nizhny Novgorod State University, 23 Gagarin avenue, Nizhny Novgorod, 603950, Russia
[2] Nizhny Novgorod State Agrotechnical University, 97 Gagarin avenue, Nizhny Novgorod, 603950, Russia

ABSTRACT

In this paper we introduce an approach to increase integration rate of elements of a CMOS cross-coupled voltage controlled oscillator. In the framework of the approach we consider a heterostructure with special configuration. Several specific areas of the heterostructure should be doped by diffusion or ion implantation. Annealing of dopant and/or radiation defects should be optimized.

KEYWORDS

CMOS cross-coupled voltage controlled oscillator; optimization of manufacturing; analytical approach for prognosis

1. INTRODUCTION

An actual and intensively solving problems of solid state electronics is increasing of integration rate of elements of integrated circuits (*p*-*n*-junctions, their systems et al) [1-8]. Increasing of the integration rate leads to necessity to decrease their dimensions. To decrease the dimensions are using several approaches. They are widely using laser and microwave types of annealing of infused dopants. These types of annealing are also widely using for annealing of radiation defects, generated during ion implantation [9-17]. Using the approaches gives a possibility to increase integration rate of elements of integrated circuits through in homogeneity of technological parameters due to generating in homogenous distribution of temperature. In this situation one can obtain decreasing dimensions of elements of integrated circuits [18] with account Arrhenius law [1,3]. Another approach to manufacture elements of integrated circuits with smaller dimensions is doping of heterostructure by diffusion or ion implantation [1-3]. However in this case optimization of dopant and/or radiation defects is required [18].

In this paper we consider a heterostructure. The heterostructure consist of a substrate and several epitaxial layers. Some sections have been manufactured in the epitaxial layers. Further we consider doping of these sections by diffusion or ion implantation. The doping gives a possibility to manufacture field-effect transistors in the framework of a CMOS cross-coupled voltage controlled oscillator so as it is shown on Figs. 1. The manufacturing gives a possibility to increase density of elements of the integrator circuit [4]. After the considered doping dopant and/or radiation defects should be annealed. Framework the paper we analyzed dynamics of redistribution of dopant and/or radiation defects during their annealing. We introduce an

approach to decrease dimensions of the element. However it is necessary to complicate technological process.

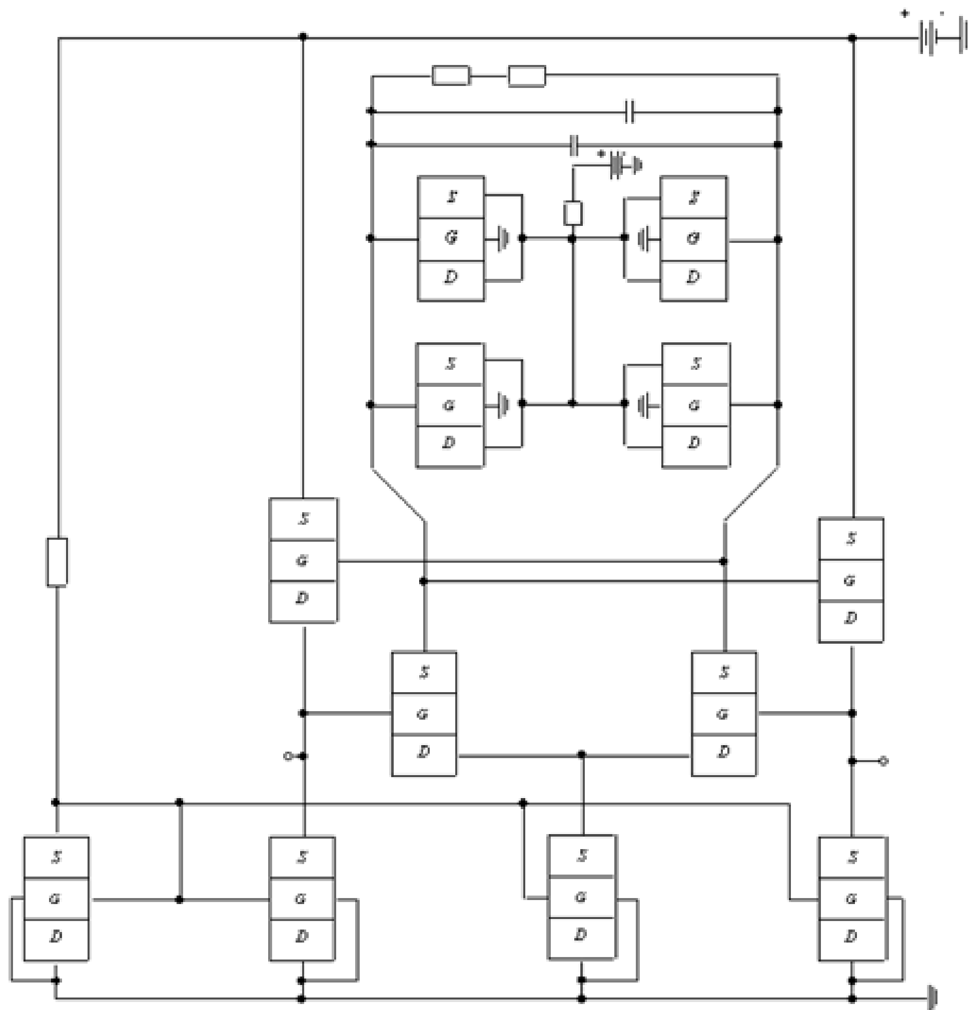

Fig. 1*a*. The considered oscillator [19]

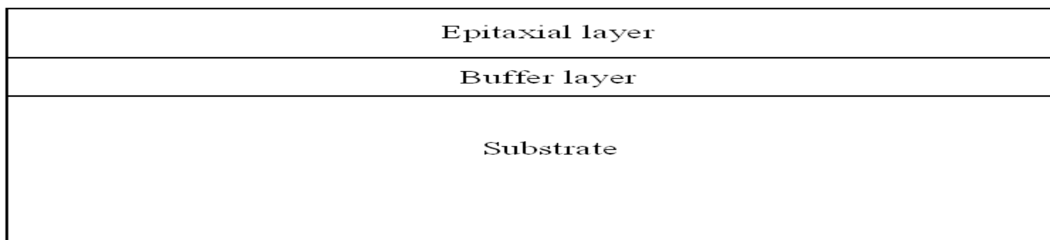

Fig. 1*b*. Heterostructure with a substrate, epitaxial layers and buffer layer (view from side)

2. METHOD OF SOLUTION

To solve our aim we determine and analyzed spatio-temporal distribution of concentration of dopant in the considered heterostructure. We determine the distribution by solving the second Fick's law in the following form [1,20-23]

$$\frac{\partial C(x,y,z,t)}{\partial t}=\frac{\partial}{\partial x}\left[D\frac{\partial C(x,y,z,t)}{\partial x}\right]+\frac{\partial}{\partial y}\left[D\frac{\partial C(x,y,z,t)}{\partial y}\right]+\frac{\partial}{\partial z}\left[D\frac{\partial C(x,y,z,t)}{\partial z}\right]+ \quad (1)$$

$$+\Omega\frac{\partial}{\partial x}\left[\frac{D_S}{kT}\nabla_S\mu_1(x,y,z,t)\int_0^{L_z}C(x,y,W,t)dW\right]+\Omega\frac{\partial}{\partial y}\left[\frac{D_S}{kT}\nabla_S\mu_1(x,y,z,t)\int_0^{L_z}C(x,y,W,t)dW\right]+$$

$$+\frac{\partial}{\partial x}\left[\frac{D_{CS}}{\bar{V}kT}\frac{\partial\mu_2(x,y,z,t)}{\partial x}\right]+\frac{\partial}{\partial y}\left[\frac{D_{CS}}{\bar{V}kT}\frac{\partial\mu_2(x,y,z,t)}{\partial y}\right]+\frac{\partial}{\partial z}\left[\frac{D_{CS}}{\bar{V}kT}\frac{\partial\mu_2(x,y,z,t)}{\partial z}\right]$$

with boundary and initial conditions

$$\left.\frac{\partial C(x,y,z,t)}{\partial x}\right|_{x=0}=0,\ \left.\frac{\partial C(x,y,z,t)}{\partial x}\right|_{x=L_x}=0,\ \left.\frac{\partial C(x,y,z,t)}{\partial y}\right|_{y=0}=0,\ \left.\frac{\partial C(x,y,z,t)}{\partial y}\right|_{x=L_y}=0,$$

$$\left.\frac{\partial C(x,y,z,t)}{\partial z}\right|_{z=0}=0,\ \left.\frac{\partial C(x,y,z,t)}{\partial z}\right|_{x=L_z}=0,\ C(x,y,z,0)=f_C(x,y,z).$$

Here $C(x,y,z,t)$ is the spatio-temporal distribution of concentration of dopant; Ω is the atomic volume of dopant; ∇_s is the symbol of surficial gradient; $\int_0^{L_z}C(x,y,z,t)dz$ is the surficial concentration of dopant on interface between layers of heterostructure (in this situation we assume, that Z-axis is perpendicular to interface between layers of heterostructure); $\mu_1(x,y,z,t)$ and $\mu_2(x,y,z,t)$ are the chemical potential due to the presence of mismatch-induced stress and porosity of material; D and D_S are the coefficients of volumetric and surficial diffusions. Values of dopant diffusions coefficients depends on properties of materials of heterostructure, speed of heating and cooling of materials during annealing and spatio-temporal distribution of concentration of dopant. Dependences of dopant diffusions coefficients on parameters could be approximated by the following relations [24-26]

$$D_C=D_L(x,y,z,T)\left[1+\xi\frac{C^\gamma(x,y,z,t)}{P^\gamma(x,y,z,T)}\right]\left[1+\varsigma_1\frac{V(x,y,z,t)}{V^*}+\varsigma_2\frac{V^2(x,y,z,t)}{(V^*)^2}\right],$$

$$D_S=D_{SL}(x,y,z,T)\left[1+\xi_S\frac{C^\gamma(x,y,z,t)}{P^\gamma(x,y,z,T)}\right]\left[1+\varsigma_1\frac{V(x,y,z,t)}{V^*}+\varsigma_2\frac{V^2(x,y,z,t)}{(V^*)^2}\right]. \quad (2)$$

Here $D_L(x,y,z,T)$ and $D_{LS}(x,y,z,T)$ are the spatial (due to accounting all layers of heterostruicture) and temperature (due to Arrhenius law) dependences of dopant diffusion coefficients; T is the temperature of annealing; $P(x,y,z,T)$ is the limit of solubility of dopant; parameter γ depends on properties of materials and could be integer in the following interval $\gamma\in[1,3]$ [24]; $V(x,y,z,t)$ is the spatio-temporal distribution of concentration of radiation vacancies; V^* is the equilibrium distribution of vacancies. Concentrational dependence of dopant diffusion coefficient has been described in details in [24]. Spatio-temporal distributions of concentration of point radiation defects have been determined by solving the following system of equations [20-23,25,26]

$$\frac{\partial I(x,y,z,t)}{\partial t}=\frac{\partial}{\partial x}\left[D_I(x,y,z,T)\frac{\partial I(x,y,z,t)}{\partial x}\right]+\frac{\partial}{\partial y}\left[D_I(x,y,z,T)\frac{\partial I(x,y,z,t)}{\partial y}\right]+$$

$$+\frac{\partial}{\partial z}\left[D_I(x,y,z,T)\frac{\partial I(x,y,z,t)}{\partial z}\right]-k_{I,I}(x,y,z,T)\,I^2(x,y,z,t)-k_{I,V}(x,y,z,T)\times$$

$$\times I(x,y,z,t)V(x,y,z,t)+\Omega\frac{\partial}{\partial x}\left[\frac{D_{IS}}{kT}\nabla_S\mu(x,y,z,t)\int_0^{L_z}I(x,y,W,t)dW\right]+$$

$$+\Omega\frac{\partial}{\partial y}\left[\frac{D_{IS}}{kT}\nabla_S\mu(x,y,z,t)\int_0^{L_z}I(x,y,W,t)dW\right]+\frac{\partial}{\partial x}\left[\frac{D_{IS}}{\bar{V}kT}\frac{\partial\mu_2(x,y,z,t)}{\partial x}\right]+$$

$$+\frac{\partial}{\partial y}\left[\frac{D_{IS}}{\bar{V}kT}\frac{\partial\mu_2(x,y,z,t)}{\partial y}\right]+\frac{\partial}{\partial z}\left[\frac{D_{IS}}{\bar{V}kT}\frac{\partial\mu_2(x,y,z,t)}{\partial z}\right] \quad (3)$$

$$\frac{\partial V(x,y,z,t)}{\partial t}=\frac{\partial}{\partial x}\left[D_V(x,y,z,T)\frac{\partial V(x,y,z,t)}{\partial x}\right]+\frac{\partial}{\partial y}\left[D_V(x,y,z,T)\frac{\partial V(x,y,z,t)}{\partial y}\right]+$$

$$+\frac{\partial}{\partial z}\left[D_V(x,y,z,T)\frac{\partial V(x,y,z,t)}{\partial z}\right]-k_{V,V}(x,y,z,T)V^2(x,y,z,t)-k_{I,V}(x,y,z,T)\times$$

$$\times I(x,y,z,t)V(x,y,z,t)+\Omega\frac{\partial}{\partial x}\left[\frac{D_{VS}}{kT}\nabla_S\mu(x,y,z,t)\int_0^{L_z}V(x,y,W,t)dW\right]+$$

$$+\Omega\frac{\partial}{\partial y}\left[\frac{D_{VS}}{kT}\nabla_S\mu(x,y,z,t)\int_0^{L_z}V(x,y,W,t)dW\right]+\frac{\partial}{\partial x}\left[\frac{D_{VS}}{\bar{V}kT}\frac{\partial\mu_2(x,y,z,t)}{\partial x}\right]+$$

$$+\frac{\partial}{\partial y}\left[\frac{D_{VS}}{\bar{V}kT}\frac{\partial\mu_2(x,y,z,t)}{\partial y}\right]+\frac{\partial}{\partial z}\left[\frac{D_{VS}}{\bar{V}kT}\frac{\partial\mu_2(x,y,z,t)}{\partial z}\right]$$

with boundary and initial conditions

$$\left.\frac{\partial I(x,y,z,t)}{\partial x}\right|_{x=0}=0,\ \left.\frac{\partial I(x,y,z,t)}{\partial x}\right|_{x=L_x}=0,\ \left.\frac{\partial I(x,y,z,t)}{\partial y}\right|_{y=0}=0,\ \left.\frac{\partial I(x,y,z,t)}{\partial y}\right|_{y=L_y}=0,$$

$$\left.\frac{\partial I(x,y,z,t)}{\partial z}\right|_{z=0}=0,\ \left.\frac{\partial I(x,y,z,t)}{\partial z}\right|_{z=L_z}=0,\ \left.\frac{\partial V(x,y,z,t)}{\partial x}\right|_{x=0}=0,\ \left.\frac{\partial V(x,y,z,t)}{\partial x}\right|_{x=L_x}=0,$$

$$\left.\frac{\partial V(x,y,z,t)}{\partial y}\right|_{y=0}=0,\ \left.\frac{\partial V(x,y,z,t)}{\partial y}\right|_{y=L_y}=0,\ \left.\frac{\partial V(x,y,z,t)}{\partial z}\right|_{z=0}=0,\ \left.\frac{\partial V(x,y,z,t)}{\partial z}\right|_{z=L_z}=0, \quad (4)$$

$$I(x,y,z,0)=f_I(x,y,z),\ V(x,y,z,0)=f_V(x,y,z),\ V(x_1+V_nt,y_1+V_nt,z_1+V_nt,t)=V_\infty\left(1+\frac{2\ell\omega}{kT\sqrt{x_1^2+y_1^2+z_1^2}}\right).$$

Here $I(x,y,z,t)$ is the spatio-temporal distribution of concentration of radiation interstitials; I^* is the equilibrium distribution of interstitials; $D_I(x,y,z,T)$, $D_V(x,y,z,T)$, $D_{IS}(x,y,z,T)$, $D_{VS}(x,y,z,T)$ are the coefficients of volumetric and surficial diffusions of interstitials and vacancies, respectively; terms $V^2(x,y,z,t)$ and $I^2(x,y,z,t)$ correspond to generation of divacancies and diinterstitials, respectively (see, for example, [26] and appropriate references in this book); $k_{I,V}(x,y,z,T)$, $k_{I,I}(x,y,z,T)$ and $k_{V,V}(x,y,z,T)$ are the parameters of recombination of point radiation defects and generation of their complexes; k is the Boltzmann constant; $\omega = a^3$, a is the interatomic distance; ℓ is the specific surface energy. To account porosity of buffer layers we assume, that porous are approximately cylindrical with average values $r=\sqrt{x_1^2+y_1^2}$ and z_1 before annealing [23]. With time small pores decomposing on vacancies. The vacancies absorbing by larger pores [27]. With time large pores became larger due to absorbing the vacancies and became more spherical [27]. Distribution of concentration of vacancies in heterostructure, existing due to porosity, could be determined by summing on all pores, i.e.

$$V(x,y,z,t)=\sum_{i=0}^{l}\sum_{j=0}^{m}\sum_{k=0}^{n}V_p(x+i\,\alpha,y+j\,\beta,z+k\,\chi,t),\ R=\sqrt{x^2+y^2+z^2}\ .$$

`

Here α, β and χ are the average distances between centers of pores in directions x, y and z; l, m and n are the quantity of pores inappropriate directions.

Spatio-temporal distributions of divacancies $\Phi_V\ (x,y,z,t)$ and diinterstitials $\Phi_I\ (x,y,z,\ t)$ could be determined by solving the following system of equations [25,26]

$$\frac{\partial\Phi_I(x,y,z,t)}{\partial t}=\frac{\partial}{\partial x}\left[D_{\Phi_I}(x,y,z,T)\frac{\partial\Phi_I(x,y,z,t)}{\partial x}\right]+\frac{\partial}{\partial y}\left[D_{\Phi_I}(x,y,z,T)\frac{\partial\Phi_I(x,y,z,t)}{\partial y}\right]+$$
$$+\frac{\partial}{\partial z}\left[D_{\Phi_I}(x,y,z,T)\frac{\partial\Phi_I(x,y,z,t)}{\partial z}\right]+\Omega\frac{\partial}{\partial x}\left[\frac{D_{\Phi_I S}}{kT}\nabla_S\mu_1(x,y,z,t)\int_0^{L_z}\Phi_I(x,y,W,t)dW\right]+$$
$$+\Omega\frac{\partial}{\partial y}\left[\frac{D_{\Phi_I S}}{kT}\nabla_S\mu_1(x,y,z,t)\int_0^{L_z}\Phi_I(x,y,W,t)dW\right]+k_{I,I}(x,y,z,T)I^2(x,y,z,t)+k_I(x,y,z,T)I(x,y,z,t)+$$
$$+\frac{\partial}{\partial x}\left[\frac{D_{\Phi_I S}}{\bar{V}kT}\frac{\partial\mu_2(x,y,z,t)}{\partial x}\right]+\frac{\partial}{\partial y}\left[\frac{D_{\Phi_I S}}{\bar{V}kT}\frac{\partial\mu_2(x,y,z,t)}{\partial y}\right]+\frac{\partial}{\partial z}\left[\frac{D_{\Phi_I S}}{\bar{V}kT}\frac{\partial\mu_2(x,y,z,t)}{\partial z}\right]\quad(5)$$

$$\frac{\partial\Phi_V(x,y,z,t)}{\partial t}=\frac{\partial}{\partial x}\left[D_{\Phi_V}(x,y,z,T)\frac{\partial\Phi_V(x,y,z,t)}{\partial x}\right]+\frac{\partial}{\partial y}\left[D_{\Phi_V}(x,y,z,T)\frac{\partial\Phi_V(x,y,z,t)}{\partial y}\right]+$$
$$+\frac{\partial}{\partial z}\left[D_{\Phi_V}(x,y,z,T)\frac{\partial\Phi_V(x,y,z,t)}{\partial z}\right]+\Omega\frac{\partial}{\partial x}\left[\frac{D_{\Phi_V S}}{kT}\nabla_S\mu_1(x,y,z,t)\int_0^{L_z}\Phi_V(x,y,W,t)dW\right]+$$
$$+\Omega\frac{\partial}{\partial y}\left[\frac{D_{\Phi_V S}}{kT}\nabla_S\mu_1(x,y,z,t)\int_0^{L_z}\Phi_V(x,y,W,t)dW\right]+k_{V,V}(x,y,z,T)\,V^2(x,y,z,t)+k_V(x,y,z,T)\,V(x,y,z,t)+$$
$$+\frac{\partial}{\partial x}\left[\frac{D_{\Phi_V S}}{\bar{V}kT}\frac{\partial\mu_2(x,y,z,t)}{\partial x}\right]+\frac{\partial}{\partial y}\left[\frac{D_{\Phi_V S}}{\bar{V}kT}\frac{\partial\mu_2(x,y,z,t)}{\partial y}\right]+\frac{\partial}{\partial z}\left[\frac{D_{\Phi_V S}}{\bar{V}kT}\frac{\partial\mu_2(x,y,z,t)}{\partial z}\right]$$

with boundary and initial conditions

$$\left.\frac{\partial\Phi_I(x,y,z,t)}{\partial x}\right|_{x=0}=0,\ \left.\frac{\partial I(x,y,z,t)}{\partial x}\right|_{x=L_x}=0,\ \left.\frac{\partial I(x,y,z,t)}{\partial y}\right|_{y=0}=0,\ \left.\frac{\partial I(x,y,z,t)}{\partial y}\right|_{y=L_y}=0,$$
$$\left.\frac{\partial\Phi_I(x,y,z,t)}{\partial z}\right|_{z=0}=0,\ \left.\frac{\partial I(x,y,z,t)}{\partial z}\right|_{z=L_z}=0,\ \left.\frac{\partial\Phi_V(x,y,z,t)}{\partial x}\right|_{x=0}=0,\ \left.\frac{\partial V(x,y,z,t)}{\partial x}\right|_{x=L_x}=0,$$
$$\left.\frac{\partial V(x,y,z,t)}{\partial y}\right|_{y=0}=0,\ \left.\frac{\partial V(x,y,z,t)}{\partial y}\right|_{y=L_y}=0,\ \left.\frac{\partial V(x,y,z,t)}{\partial z}\right|_{z=0}=0,\ \left.\frac{\partial\Phi_V(x,y,z,t)}{\partial z}\right|_{z=L_z}=0,$$

$$\Phi_I\,(x,y,z,0)=f_{\Phi I}\,(x,y,z),\ \Phi_V\,(x,y,z,0)=f_{\Phi V}\,(x,y,z).\quad(6)$$

Here $D_{\Phi I}(x,y,z,T)$, $D_{\Phi V}(x,y,z,T)$, $D_{\Phi IS}\,(x,y,z,T)$ and $D_{\Phi VS}(x,y,z,T)$ are the coefficients of volumetric and surficial diffusions of complexes of radiation defects; $k_I(x,y,z,T)$ and $k_V(x,y,z,T)$ are the parameters of decay of complexes of radiation defects.

Chemical potential μ_1 in Eq.(1) could be determine by the following relation [20]

$$\mu_1=E(z)\Omega\sigma_{ij}\,[u_{ij}(x,y,z,t)+u_{ji}(x,y,z,t)]/2, \tag{7}$$

where $E(z)$ is the Young modulus, σ_{ij} is the stress tensor; $u_{ij}=\frac{1}{2}\left(\frac{\partial u_i}{\partial x_j}+\frac{\partial u_j}{\partial x_i}\right)$ is the deformation tensor; u_i, u_j are the components $u_x(x,y,z,t)$, $u_y(x,y,z,t)$ and $u_z(x,y,z,t)$ of the displacement vector $\vec{u}(x,y,z,t)$; x_i, x_j are the coordinate x, y, z. The Eq. (3) could be transform to the following form

$$\mu\left(x,y,z,t\right)=E\left(z\right)\frac{\Omega}{2}\left[\frac{\partial u_i(x,y,z,t)}{\partial x_j}+\frac{\partial u_j(x,y,z,t)}{\partial x_i}\right]\left\{\frac{1}{2}\left[\frac{\partial u_i(x,y,z,t)}{\partial x_j}+\frac{\partial u_j(x,y,z,t)}{\partial x_i}\right]-\right.$$

$$\left.-\varepsilon_0\delta_{ij}+\frac{\sigma(z)\delta_{ij}}{1-2\sigma(z)}\left[\frac{\partial u_k(x,y,z,t)}{\partial x_k}-3\varepsilon_0\right]-K(z)\beta(z)[T(x,y,z,t)-T_0]\,\delta_{ij}\right\},$$

where σ is Poisson coefficient; $\varepsilon_0=(a_s\text{-}a_{EL})/a_{EL}$ is the mismatch parameter; a_s, a_{EL} are lattice distances of the substrate and the epitaxial layer; K is the modulus of uniform compression; β is the coefficient of thermal expansion; T_r is the equilibrium temperature, which coincide (for our case) with room temperature. Components of displacement vector could be obtained by solution of the following equations [21]

$$\rho\left(z\right)\frac{\partial^2 u_x(x,y,z,t)}{\partial t^2}=\frac{\partial\sigma_{xx}(x,y,z,t)}{\partial x}+\frac{\partial\sigma_{xy}(x,y,z,t)}{\partial y}+\frac{\partial\sigma_{xz}(x,y,z,t)}{\partial z}$$

$$\rho\left(z\right)\frac{\partial^2 u_y(x,y,z,t)}{\partial t^2}=\frac{\partial\sigma_{yx}(x,y,z,t)}{\partial x}+\frac{\partial\sigma_{yy}(x,y,z,t)}{\partial y}+\frac{\partial\sigma_{yz}(x,y,z,t)}{\partial z}$$

$$\rho\left(z\right)\frac{\partial^2 u_z(x,y,z,t)}{\partial t^2}=\frac{\partial\sigma_{zx}(x,y,z,t)}{\partial x}+\frac{\partial\sigma_{zy}(x,y,z,t)}{\partial y}+\frac{\partial\sigma_{zz}(x,y,z,t)}{\partial z},$$

where $\sigma_{ij}=\frac{E(z)}{2[1+\sigma(z)]}\left[\frac{\partial u_i(x,y,z,t)}{\partial x_j}+\frac{\partial u_j(x,y,z,t)}{\partial x_i}-\frac{\delta_{ij}}{3}\frac{\partial u_k(x,y,z,t)}{\partial x_k}\right]+\delta_{ij}\frac{\partial u_k(x,y,z,t)}{\partial x_k}\times$ $\times K(z)-\beta(z)K(z)[T(x,y,z,t)-T_r]$, $\rho(z)$ is the density of materials of heterostructure, δ_i is the Kronecker symbol. With account the relation for σ_{ij} last system of equation could be written as

$$\rho(z)\frac{\partial^2 u_x(x,y,z,t)}{\partial t^2}=\left\{K(z)+\frac{5E(z)}{6[1+\sigma(z)]}\right\}\frac{\partial^2 u_x(x,y,z,t)}{\partial x^2}+\left\{K(z)-\frac{E(z)}{3[1+\sigma(z)]}\right\}\frac{\partial^2 u_y(x,y,z,t)}{\partial x\partial y}+$$

$$+\frac{E(z)}{2[1+\sigma(z)]}\left[\frac{\partial^2 u_y(x,y,z,t)}{\partial y^2}+\frac{\partial^2 u_z(x,y,z,t)}{\partial z^2}\right]+\left[K(z)+\frac{E(z)}{3[1+\sigma(z)]}\right]\frac{\partial^2 u_z(x,y,z,t)}{\partial x\partial z}-\frac{\partial T(x,y,z,t)}{\partial x}\times$$

$$\times K(z)\beta(z)$$

$$\rho(z)\frac{\partial^2 u_y(x,y,z,t)}{\partial t^2}=\frac{E(z)}{2[1+\sigma(z)]}\left[\frac{\partial^2 u_y(x,y,z,t)}{\partial x^2}+\frac{\partial^2 u_x(x,y,z,t)}{\partial x\partial y}\right]-K(z)\,\beta(z)\frac{\partial T(x,y,z,t)}{\partial y}+$$

$$+\frac{\partial}{\partial z}\left\{\frac{E(z)}{2[1+\sigma(z)]}\left[\frac{\partial u_y(x,y,z,t)}{\partial z}+\frac{\partial u_z(x,y,z,t)}{\partial y}\right]\right\}+\frac{\partial^2 u_y(x,y,z,t)}{\partial y^2}\left\{\frac{5E(z)}{12[1+\sigma(z)]}+K(z)\right\}+$$

$$+\left\{K(z)-\frac{E(z)}{6[1+\sigma(z)]}\right\}\frac{\partial^2 u_y(x,y,z,t)}{\partial y\partial z}+K(z)\frac{\partial^2 u_y(x,y,z,t)}{\partial x\partial y} \tag{8}$$

$$\rho(z)\frac{\partial^2 u_z(x,y,z,t)}{\partial t^2}=\left[\frac{\partial^2 u_z(x,y,z,t)}{\partial x^2}+\frac{\partial^2 u_z(x,y,z,t)}{\partial y^2}+\frac{\partial^2 u_x(x,y,z,t)}{\partial x\partial z}+\frac{\partial^2 u_y(x,y,z,t)}{\partial y\partial z}\right]\times$$

$$\times\frac{E(z)}{2[1+\sigma(z)]}+\frac{\partial}{\partial z}\left\{K(z)\left[\frac{\partial u_x(x,y,z,t)}{\partial x}+\frac{\partial u_y(x,y,z,t)}{\partial y}+\frac{\partial u_x(x,y,z,t)}{\partial z}\right]\right\}+$$

$$+\frac{1}{6}\frac{\partial}{\partial z}\left\{\frac{E(z)}{1+\sigma(z)}\left[6\frac{\partial u_z(x,y,z,t)}{\partial z}-\frac{\partial u_x(x,y,z,t)}{\partial x}-\frac{\partial u_y(x,y,z,t)}{\partial y}-\frac{\partial u_z(x,y,z,t)}{\partial z}\right]\right\}-$$

$$-K(z)\beta(z)\frac{\partial T(x,y,z,t)}{\partial z}.$$

Conditions for the system of Eq. (8) could be written in the form

$$\frac{\partial \vec{u}(0,y,z,t)}{\partial x}=0;\ \frac{\partial \vec{u}(L_x,y,z,t)}{\partial x}=0;\ \frac{\partial \vec{u}(x,0,z,t)}{\partial y}=0;\ \frac{\partial \vec{u}(x,L_y,z,t)}{\partial y}=0;$$

$$\frac{\partial \vec{u}(x,y,0,t)}{\partial z}=0;\ \frac{\partial \vec{u}(x,y,L_z,t)}{\partial z}=0;\ \vec{u}(x,y,z,0)=\vec{u}_0;\ \vec{u}(x,y,z,\infty)=\vec{u}_0.$$

We determine spatio-temporal distributions of concentrations of dopant and radiati-on defects by solving the Eqs.(1), (3) and (5) in the framework of the standard method of averaging of function corrections [28]. In the framework of this paper we determine concentration of dopant, concentrations of radiation defects and components of displacement vector by using the second-order approximation framework method of averaging of function corrections. This approximation is usually enough good approximation to make qualitative analysis and to obtain some quantitative results. All obtained results have been checked by comparison with results of numerical simulations.

3. DISCUSSION

In this section we analyzed dynamics of redistributions of dopant and radiation defects during annealing and under influence of mismatch-induced stress and modification of porosity. Typical distributions of concentrations of dopant in heterostructures are presented on Figs. 2 and 3 for diffusion and ion types of doping, respectively. These distributions have been calculated for the case, when value of dopant diffusion coefficient in doped area is larger, than in nearest areas. The figures show, that inhomogeneity of heterostructure gives us possibility to increase compactness of concentrations of dopants and at the same time to increase homogeneity of dopant distribution in doped part of epitaxial layer. However framework this approach of manufacturing of bipolar transistor it is necessary to optimize annealing of dopant and/or radiation defects. Reason of this optimization is following. If annealing time is small, the dopant did not achieve any interfaces between materials of heterostructure. In this situation one cannot find any modifications of distribution of concentration of dopant. If annealing time is large, distribution of concentration of dopant is too homogenous. We optimize annealing time in the framework of recently introduces approach [29-37]. Framework this criterion we approximate real distribution of concentration of dopant by step-wise function (see Figs. 4 and 5). Farther we determine optimal values of annealing time by minimization of the following mean-squared error

$$U=\frac{1}{L_xL_yL_z}\int_0^{L_x}\int_0^{L_y}\int_0^{L_z}[C(x,y,z,\Theta)-\psi(x,y,z)]\,d\,z\,d\,y\,d\,x, \quad (15)$$

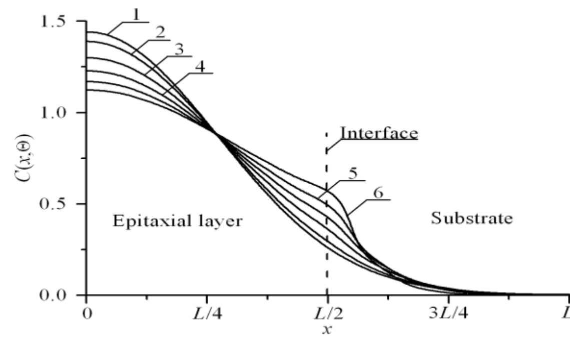

Fig. 2. Distributions of concentration of infused dopant in heterostructure from Fig. 1 in direction, which is perpendicular to interface between epitaxial layer substrate. Increasing of number of curve corresponds to increasing of difference between values of dopant diffusion coefficient in layers of heterostructure under condition, when value of dopant diffusion coefficient in epitaxial layer is larger, than value of dopant diffusion coefficient in substrate

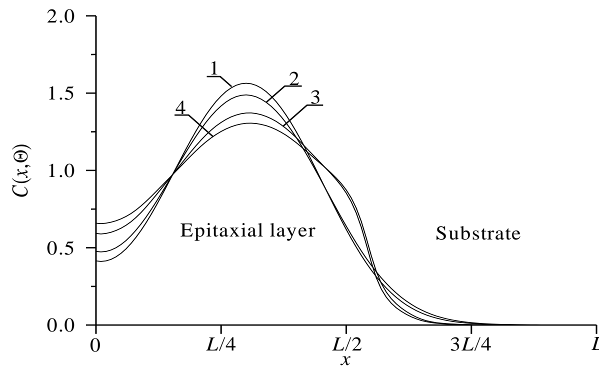

Fig. 3. Distributions of concentration of implanted dopant in heterostructure from Fig. 1 in direction, which is perpendicular to interface between epitaxial layer substrate. Curves 1 and 3 corresponds to annealing time $\Theta = 0.0048(L_x^2+L_y^2+L_z^2)/D_0$. Curves 2 and 4 corresponds to annealing time $\Theta =.0057(L_x^2+L_y^2+L_z^2)/D_0$. Curves 1 and 2 corresponds to homogenous sample. Curves 3 and 4 corresponds to heterostructure under condition, when value of dopant diffusion coefficient in epitaxial layer is larger, than value of dopant diffusion coefficient in substrate

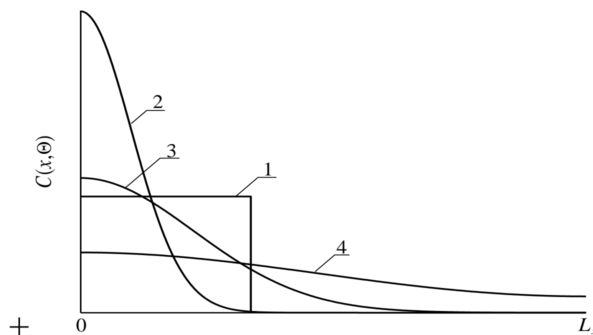

Fig. 4. Spatial distributions of dopant in heterostructure after dopant infusion. Curve 1 is idealized distribution of dopant. Curves 2-4 are real distributions of dopant for different values of annealing time. Increasing of number of curve corresponds to increasing of annealing time

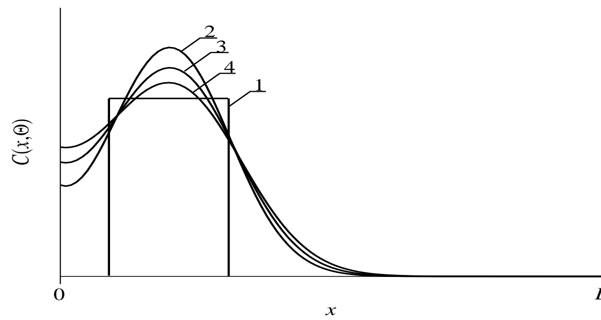

Fig. 5. Spatial distributions of dopant in heterostructure after ion implantation. Curve 1 is idealized distribution of dopant. Curves 2-4 are real distributions of dopant for different values of annealing time. Increasing of number of curve corresponds to increasing of annealing time

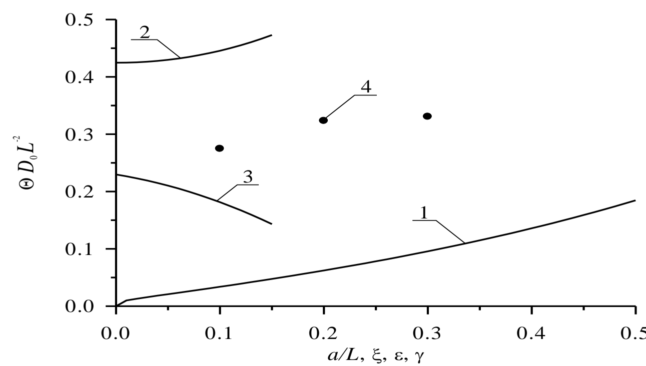

Fig. 6. Dependences of dimensionless optimal annealing time for doping by diffusion, which have been obtained by minimization of mean-squared error, on several parameters. Curve 1 is the dependence of dimensionless optimal annealing time on the relation *a/L* and $\xi = \gamma = 0$ for equal to each other values of dopant diffusion coefficient in all parts of heterostructure. Curve 2 is the dependence of dimensionless optimal annealing time on value of parameter ε for a/L=1/2 and $\xi = \gamma = 0$. Curve 3 is the dependence of dimensionless optimal annealing time on value of parameter ξ for a/L=1/2 and $\varepsilon = \gamma = 0$. Curve 4 is the dependence of dimensionless optimal annealing time on value of parameter γ for a/L=1/2 and $\varepsilon = \xi = 0$

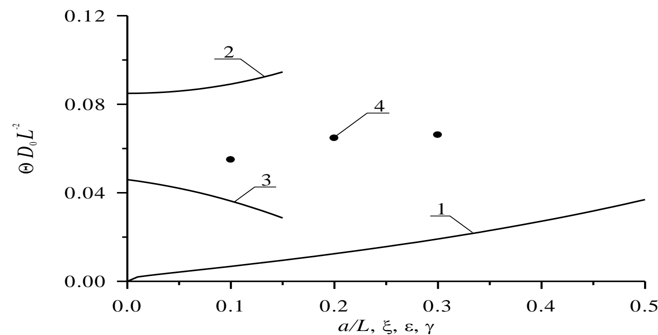

Fig.7. Dependences of dimensionless optimal annealing time for doping by ion implantation, which have been obtained by minimization of mean-squared error, on several parameters. Curve 1 is the dependence of dimensionless optimal annealing time on the relation *a/L* and $\xi = \gamma = 0$ for equal to each other values of dopant diffusion coefficient in all parts of heterostructure. Curve 2 is the dependence of dimensionless optimal annealing time on value of parameter ε for a/L=1/2 and $\xi = \gamma = 0$. Curve 3 is the dependence of dimensionless optimal annealing time on value of parameter ξ for a/L=1/2 and $\varepsilon = \gamma = 0$. Curve 4 is the dependence of dimensionless optimal annealing time on value of parameter γ for a/L=1/2 and $\varepsilon = \xi = 0$

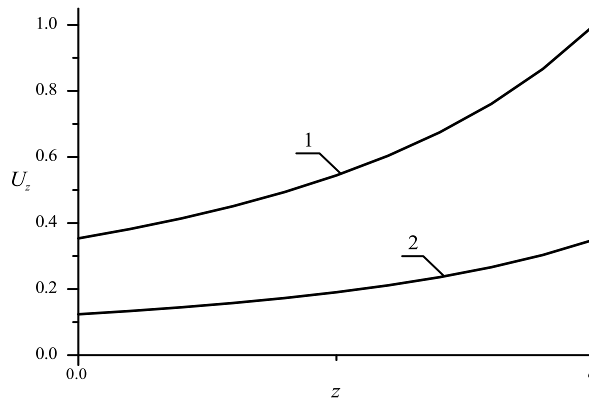

Fig. 8. Normalized dependences of component u_z of displacement vector on coordinate z for nonporous (curve 1) and porous (curve 2) epitaxial layers

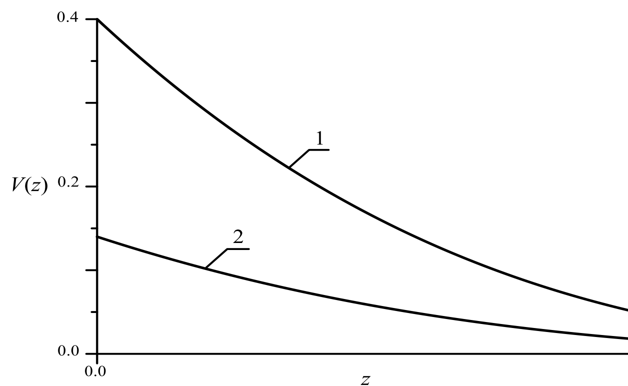

Fig. 9. Normalized dependences of vacancy concentrations on coordinate z in unstressed (curve 1) and stressed (curve 2) epitaxial layers

Farther we analyzed influence of relaxation of mechanical stress on distribution of dopant in doped areas of heterostructure. Under following condition $\varepsilon_0 < 0$ one can find compression of distribution of concentration of dopant near interface between materials of heterostructure. Contrary (at $\varepsilon_0 > 0$) one can find spreading of distribution of concentration of dopant in this area. This changing of distribution of concentration of dopant could be at least partially compensated by using laser annealing [37]. This type of annealing gives us possibility to accelerate diffusion of dopant and another processes in annealed area due to inhomogenous distribution of temperature and Arrhenius law. Accounting relaxation of mismatch-induced stress in heterostructure could leads to changing of optimal values of annealing time. At the same time modification of porosity gives us possibility to decrease value of mechanical stress. On the one hand mismatch-induced stress could be used to increase density of elements of integrated circuits. On the other hand could leads to generation dislocations of the discrepancy. Figs. 8 and 9 show distributions of concentration of vacancies in porous materials and component of displacement vector, which is perpendicular to interface between layers of heterostructure.

4. CONCLUSIONS

In this paper we introduce an approach to increase integration rate of element of a CMOS cross-coupled voltage controlled oscillator. The approach gives us possibility to decrease area of the elements with smaller increasing of the element’s thickness.

REFERENCES

[1] Lachin V.I., Savelov N.S., "Electronics", Rostov-on-Don: Phoenix, 2001.

[2] Polishscuk A., "Anadigm Programmable Analog ICs: The full range of analog electronics on a single chip. First meeting", Modern Electronics, no. 12. pp. 8-11, 2004.

[3] Volovich G., "Modern chips UM3Ch class D manufactured by firm MPS", Modern Electronics, no 2, pp. 10-17, 2006.

[4] Kerentsev A., Lanin V., "Constructive-technological features of MOSFET-transistors ", Power Electronics, no 1, pp. 34-38, 2008.

[5] Ageev A.O., Belyaev A.E., Boltovets N.S., Ivanov V.N., Konakova R.V., Kudrik Ya.Ya., Litvin P.M., Milenin V.V., Sachenko A.V., "Influence of displacement of the electron-hole equilibrium on the process of transition metals diffusion in GaAs", Semiconductors, vol. 43, no. 7, 7, pp. 897-903, 2009.

[6] Tsai J.-H., Chiu S.-Y., Lour W.-Sh., Guo D,-F.,. InGaP/GaAs/InGaAs δ-doped p-channel field-effect transistor with $p+/n^{+}/p$ camel-like gate structure, Semiconductors, vol. 43, 7, pp. 971-974, 2009.

[7] Alexandrov O.V., Zakhar'in A.O., Sobolev N.A., Shek E.I., Makoviychuk M.M., Parshin E.O., Formation of donor centers upon annealing of dysprosium- and holmium-implanted silicon, Semiconductors, vol. 32, 9, pp. 1029-1032, 1998.

[8] Ermolovich I.B., Milenin V.V., Red'ko R.A., Red'ko S.M., Features of recombination processes in CdTe films, preparing at different temperature conditions and further annealing, Semiconductors, vol. 43, 8, pp. 1016-1020, 2009.

[9] Sinsermsuksakul P., Hartman K., Kim S.B., Heo J., Sun L., Park H.H., Chakraborty R., Buonassisi T., Gordon R.G., Enhancing the efficiency of SnS solar cells via band-offset engineering with a zinc oxysulfide buffer layer, Applied Physics Letters, vol. 102, 5, pp. 053901-053905, 2013.

[10] Reynolds J.G., Reynolds C.L., Mohanta Jr.A., Muth J.F., Rowe J.E., Everitt H.O., Aspnes D.E., Shallow acceptor complexes in p-type ZnO, Applied Physics Letters, vol. 102, 15, pp. 152114-152118, 2013.

[11] Volokobinskaya N.I., Komarov I.N., Matyukhina T.V., Reshetnikov V.I., Rush A.A., Falina I.V., Yastrebov A.S., A study of technological processes in the production of high-power high-voltage bipolar transistors incorporating an array of inclusions in the collector region, Semiconductors, vol. 35, 8, pp. 1013-1017, 2001.

[12] Pankratov E.L., Bulaeva, E.A., Doping of materials during manufacture p-n-junctions and bipolar transistors. Analytical approaches to model technological approaches and ways of optimization of distributions of dopants, Reviews in Theoretical Science, vol. 1, 1, pp. 58-82, 2013.

[13] Kukushkin S.A., Osipov A.V., Romanychev A.I., Epitaxial growth of zinc oxide by the method of atomic layer deposition on SiC/Si substrates, Physics of the Solid State, vol. 58, 7, pp. 1448-1452, 2016.

[14] Trukhanov E.M., Kolesnikov A.V., Loshkarev I.D., Long-range stresses generated by misfit dislocations in epitaxial films, Russian Microelectronics, vol. 44, 8, pp. 552-558, 2015.

[15] Pankratov E.L., Bulaeva, E.A., On optimization of regimes of epitaxy from gas phase. some analytical approaches to model physical processes in reactors for epitaxy from gas phase during growth films, Reviews in Theoretical Science, vol. 3, 4, pp. 365-398, 2015.

[16] Ong K.K., Pey K.L., Lee P.S., Wee A.T.S., Wang X.C., Chong Y.F., Fabrication of p-ZnO:Na/n-ZnO:Na homojunction by surface pulsed laser irradiation, Applied Physics Letters, vol. 89, 17, pp. 172111-172114, 2006.

[17] Wang H.T., Tan L.S., Chor E.F., Pulsed laser annealing of Be-implanted GaN, Journal of Applied Physics, vol. 98, 9, pp. 094901-094905, 2006.

[18] Bykov Yu.V., Yeremeev A.G., Zharova N.A., Plotnikov I.V., Rybakov K.I., Drozdov M.N., Drozdov Yu.N., Skupov V.D., Diffusion processes in semiconductor structures during microwave annealing, Radiophysics and Quantum Electronics, vol. 43, 3, pp. 836-843 2003.

[19] Haramkar G., Patil R.P., Andankar R. A 2.4 GHZ fully integrated LC VCO design using 130 NM CMOS technology. International Journal of Microelectronics Engineering. **Vol. 2** (4). P. 1-9 (2016).

[20] Zhang Y.W., Bower A.F., Three dimensional finite element analysis of the evolution of voids and thin films by strain and electromigration induced surface diffusion, Journal of the Mechanics and Physics of Solids, vol. 47, 11, pp. 2273-2297, 1999.

[21] Landau L.D., Lefshits E.M., Theoretical physics: Theory of elasticity, Moscow: Physmatlit, 2001.

[22] Kitayama M., Narushima T., Carter W.C., Cannon R.M., Glaeser A.M., "The Wulff shape of alumina: I, modeling the kinetics of morphological evolution," J. Am. Ceram. Soc., vol. 83, no. 10, pp. 2561-2571, 2000; Kitayama M., Narushima T., Glaeser A.M., "The Wulff shape of Alumina: II, experimental measurements of pore shape evolution rates", J. Am. Ceram. Soc., vol. 83, no, 10, pp. 2572-2583, 2000.

[23] Cheremskoy P.G., Slesov V.V., Betekhtin, V.I., Pore in solid bodies, Moscow: Energoatomizdat, 1990.

[24] Gotra Z.Yu., Technology of microelectronic devices, Moscow: Radio and communication, 1991.

[25] Fahey P.M., Griffin P.B., Plummer J.D., Point defects and dopant diffusion in silicon, Reviewers in Modern Physics, vol. 61, 2, pp. 289-388, 1989.

[26] Vinetskiy V.L., Kholodar' G.A., Radiative physics of semiconductors, Kiev: Naukova Dumka, 1979.

[27] Mynbaeva M.G., Mokhov E.N., Lavrent'ev A.A., Mynbaev K.D., High-temperature diffusion doping of porous silicon carbide, Technical Physics Letters, vol. 34, 17, pp. 13, 2008.

[28] Sokolov Yu.D., About the definition of dynamic forces in the mine lifting, Applied Mechanics, vol. 1, 1, pp. 23-35, 1955.

[29] Pankratov E.L., Dopant diffusion dynamics and optimal diffusion time as influenced by diffusion-coefficient nonuniformity, Russian Microelectronics, vol. 36, 1, pp. 33-39, 2007.

[30] Pankratov E.L., Redistribution of dopant during annealing of radiative defects in a multilayer structure by laser scans for production an implanted-junction rectifiers, International Journal of Nanoscience, vol. 7, 4-5, pp. 187-197, 2008.

[31] Pankratov E.L., Bulaeva, E.A., Doping of materials during manufacture p-n-junctions and bipolar transistors. Analytical approaches to model technological approaches and ways of optimization of distributions of dopants Reviews in Theoretical Science, vol. 1, 1, pp. 58-82, 2013.

[32] Pankratov E.L., Bulaeva, E.A., Decreasing of quantity of radiation defects in an implanted-junction rectifiers by using overlayers, International Journal of Micro-Nano Scale Transport, vol. 3, 3, pp. 119-130, 2012.

[33] Pankratov E.L., Bulaeva, E.A., Optimization of manufacturing of emitter-coupled logic to decrease surface of chip, International Journal of Modern Physics B, vol. 29, 5, pp. 1550023-1-1550023-12, 2015.

[34] Pankratov E.L., On approach to optimize manufacturing of bipolar heterotransistors framework circuit of an operational amplifier to increase their integration rate, Journal of Computational and Theoretical Nanoscience, vol. 14, 10, pp. 4885-4899, 2017.

[35] Pankratov E.L., Bulaeva, E.A., An approach to increase the integration rate of planar drift heterobipolar transistors, Materials science in semiconductor processing, vol. 34, pp. 260-268, 2015.

[36] Pankratov E.L., Bulaeva, E.A., An approach to manufacture of bipolar transistors in thin film structures. On the method of optimization, International Journal of Micro-Nano Scale Transport, vol. 4, 1, pp. 17-31, 2014.

[37] Pankratov E.L., Bulaeva, E.A., An analytical approach for analysis and optimization of formation of field-effect heterotransistors, Multidiscipline modeling in materials and structures, vol. 12, 4, pp. 578-604, 2016.